

Coupling of Nonconforming Finite Elements and Boundary Elements II: A Posteriori Estimates and Adaptive Mesh-Refinement

C. Carstensen and S. A. Funken, Kiel

Received January 26, 1998; revised February 10, 1999

Abstract

The coupling of nonconforming finite element and boundary element methods was established in Part I of this paper, where quasi-optimal a priori error estimates are provided. In the second part, we establish sharp a posteriori error estimates and so justify adaptive mesh-refining algorithms for the efficient numerical treatment of transmission problems with the Laplacian in unbounded domains.

AMS Subject Classifications: 65N38, 65N15, 65R20, 45L10.

Key Words: Coupling of finite elements and boundary elements, nonconforming finite elements, adaptive algorithms, a posteriori error estimates.

1. Introduction

A model transmission problem was rewritten in terms of boundary integral operators in the first part [8], subsequently referred to as Part I. In addition to the conditions stated there, we assume that the domain $\Omega \subset \mathbb{R}^2$ is simply connected and suppose that the prescribed jumps are slightly more regular, namely, $u_0 \in H^1(\Gamma)$ and $t_0 \in L^2(\Gamma)$. The continuous problem can be recast as follows: Find $(u, \xi, \phi) \in H^1(\Omega) \times H^{1/2}(\Gamma) \times H^{-1/2}(\Gamma)/\mathbb{R}$ satisfying, for all $(v, \theta, \psi) \in H^1(\Omega) \times H^{1/2}(\Gamma) \times H^{-1/2}(\Gamma)/\mathbb{R}$,

$$\begin{aligned} (\mathcal{A}(Du), Dv) - \langle \phi, v \rangle &= (f, v) + \langle t_0, v \rangle, \\ -2\langle u, \psi \rangle - \langle \mathcal{V}\phi, \psi \rangle + \langle (\mathcal{K} + 1)\xi, \psi \rangle &= -2\langle u_0, \psi \rangle, \\ \langle (\mathcal{K}^* + 1)\phi, \theta \rangle + \langle \mathcal{W}\xi, \theta \rangle &= 0. \end{aligned} \tag{1.1}$$

We recall from Part I that (\cdot, \cdot) is the scalar product in $L^2(\Omega)$, and $\langle \cdot, \cdot \rangle$ denotes the $L^2(\Gamma)$ -duality. The boundary integral operators involve the single layer potential \mathcal{V} , the double layer potential \mathcal{K} , its dual \mathcal{K}^* , and the hypersingular operator \mathcal{W} as defined in Section 2 of Part I. The capacity of Γ is assumed smaller than one, e.g., if Ω is scaled to belong to the unit ball.

The discretisation relies on a regular triangulation \mathcal{T} of the domain Ω and an induced decomposition \mathcal{G} of the polygonal boundary Γ with \mathcal{G} -piecewise constant resp. continuous and \mathcal{G} -piecewise affine spline functions $S^0(\mathcal{G})$ resp. $S^1(\mathcal{G})$. The lowest order nonconforming Crouzeix–Raviart finite element space $S^{NC}(\mathcal{T})$ consists of \mathcal{T} -piecewise affine functions that are continuous at the midpoints \mathcal{M} of edges \mathcal{E} . The \mathcal{T} -piecewise application of differential operators is denoted by a subscript \mathcal{T} , e.g., $D_{\mathcal{T}}$ is given by $(D_{\mathcal{T}}f)|_T = D(f|_T)$ on $T \in \mathcal{T}$ and $f \in H^1(\mathcal{T}) := \{g \in L^2(\Omega) : \forall T \in \mathcal{T}, f|_T \in H^1(T)\}$. Then the discrete problem can be written as in Remark 4 in Part I: *Find $(U, \Xi, \Phi) \in S^{NC}(\mathcal{T}) \times S^1(\mathcal{G})/\mathbb{R} \times S^0(\mathcal{G})$ satisfying, for all $(V, \Theta, \Psi) \in S^{NC}(\mathcal{T}) \times S^1(\mathcal{G})/\mathbb{R} \times S^0(\mathcal{G})$,*

$$\begin{aligned} 3(\mathcal{A}(D_{\mathcal{T}}U), D_{\mathcal{T}}V) - \langle \Phi, V \rangle &= (f, v) + \langle t_0, V \rangle, \\ -2\langle U, \Psi \rangle - \langle \mathcal{V}\Phi, \Psi \rangle + \langle (\mathcal{K} + 1)\Xi, \Psi \rangle &= -2\langle u_0, \Psi \rangle, \\ \langle (\mathcal{K}^* + 1)\Phi, \Theta \rangle + \langle \mathcal{W}\Xi, \Theta \rangle &= 0. \end{aligned} \quad (1.2)$$

In Part I, we showed equivalence of a model interface problem with (1.1), unique existence of solutions as well the sharp a priori error estimate

$$\begin{aligned} \|D_{\mathcal{T}}(u - U)\|_{L^2(\Omega)} \leq C \left(\|h_{\mathcal{T}}D^2u\|_{L^2(\Omega)} + \|h_{\mathcal{T}}\operatorname{div}A(Du)\|_{L^2(\Omega)} \right. \\ \left. + \operatorname{dist}_{H^{-1/2}(\Gamma)}(\mathcal{S}u|_{\Gamma} - t_0; S^0(\mathcal{G})) \right). \end{aligned}$$

It is the aim of Part II to establish some local error indicator $\eta(T)$, $T \in \mathcal{T}$, such that we have the reliable error estimate

$$\|D_{\mathcal{T}}(u - U)\|_{L^2(\Omega)}^2 \leq C \sum_{T \in \mathcal{T}} \eta(T)^2. \quad (1.3)$$

Moreover, for uniform meshes at the boundary, we have generically the reverse inequality which verifies efficiency of the a posteriori error bound. Therefore, we may base heuristic mesh-refining algorithms on (1.3) and so design an adaptive scheme which has proved to be efficient in numerical examples reported below.

The rest of Part II is organised as follows. In Section 2 we specify notation and further assumptions on the above problems (following essentially [8]). The a posteriori error estimate is stated and proved in Section 3 while its efficiency is analysed in Section 4. The corresponding adaptive mesh-refining algorithm and implementation is outlined in Section 5. Numerical examples illustrate the efficiency of the adaptive coupling scheme in Section 6.

2. A Posteriori Error Estimate

Let (u, ξ, ϕ) solve (1.1) and define and $\sigma := \mathcal{A}(Du)$. Given a solution (U, Ξ, Φ)

to (1.2), define $\Sigma := \mathcal{A}(D_{\mathcal{T}}U)$ and set $J_n, J_\tau \in L^2(\cup\mathcal{E})$, on each edge $E \in \mathcal{E}$,

$$J_n|_E := \begin{cases} (\Sigma_T - \Sigma_{T'}) \cdot n_E & \text{if } E \not\subset \Gamma, \\ \Sigma \cdot n_E - \Phi - t_0 & \text{if } E \subset \Gamma, \end{cases} \quad (2.1)$$

$$J_\tau|_E := \begin{cases} (D_{\mathcal{T}}U|_T - D_{\mathcal{T}}U|_{T'}) \cdot \tau_E & \text{if } E \not\subset \Gamma, \\ 2D_{\mathcal{T}}U|_T \cdot \tau_E - \partial/\partial s(2u_0 \\ \quad + (\mathcal{K} + 1)\Xi - \nu\Phi) & \text{if } E \subset \Gamma. \end{cases} \quad (2.2)$$

Here, n_E denotes the normal and τ_E the tangential unit vector along the edge E . In the first cases of (2.1) resp. (2.), T and T' denote two neighbouring elements that share the edge E . The local mesh-sizes $h_{\mathcal{T}} \in L^\infty(\Omega)$ and $h_{\mathcal{E}} \in L^\infty(\cup\mathcal{E})$ are piecewise constant functions with $(h_{\mathcal{T}})|_T := \text{diam}(T)$, $T \in \mathcal{T}$, and $(h_{\mathcal{E}})|_E := \text{diam}(E)$, $E \in \mathcal{E}$.

Theorem 1. *There exists a positive constant C which depends only on c_θ and the simply connected domain Ω , such that there holds*

$$\begin{aligned} & \|Du - D_{\mathcal{T}}U\|_{L^2(\Omega)}^2 + \|\phi - \Phi\|_{H^{-1/2}(\Gamma)}^2 + \|\xi - \Xi\|_{H^{1/2}(\Gamma)/\mathbb{R}}^2 \\ & \leq C \left\{ \sum_{T \in \mathcal{T}} h_T^2 \int_T |f + \text{div}_{\mathcal{T}}\Sigma|^2 dx + \sum_{E \in \mathcal{E}} h_E (\|J_n\|_{L^2(E)}^2 + \|J_\tau\|_{L^2(E)}^2) \right. \\ & \quad \left. + \sum_{E \in \mathcal{G}} h_E \|\mathcal{W}\Xi + (\mathcal{K}^* + 1)\Phi\|_{L^2(E)}^2 \right\}. \quad (2.3) \end{aligned}$$

Proof: Let $e := u - U$, $\epsilon := \phi - \Phi \in H^{-1/2}(\Gamma)$, and $\delta := \xi - \Xi \in H^{1/2}(\Gamma)$. As in Part I [8], we define

$$\rho_0 := -2e - \nu\epsilon + (\mathcal{K} + 1)\delta \perp S^0(\mathcal{G}), \quad (2.4)$$

$$\rho_1 := (\mathcal{K}^* + 1)\epsilon + \mathcal{W}\delta \perp S^1(\mathcal{G})/\mathbb{R}, \quad (2.5)$$

where \perp denotes orthogonality in $L^2(\Gamma)$. (See [8] for details, in particular for the fact that the continuous version of (1.1) is solved by $(u, \xi, \phi, 0)$, and so we have L^2 -orthogonality of the residuals ρ_0 and ρ_1 to the test functions.)

We adopt arguments from [2, 3, 5, 10, 13, 14] and consider a Helmholtz decompositions of both $D_{\mathcal{T}}e$ and $\sigma - \Sigma$. Notice that

$$g(z) := -\frac{1}{2\pi} \int_{\Gamma} \delta(\zeta) \frac{\partial}{\partial n_\zeta} \log |z - \zeta| ds_\zeta + \frac{1}{2\pi} \int_{\Gamma} \epsilon(\zeta) \log |z - \zeta| ds_\zeta \quad (z \in \Omega) \quad (2.6)$$

defines a function $g \in H^1(\Omega)$ with trace

$$g|_{\Gamma} = \frac{1}{2} \{(\mathcal{K} + 1)\delta - \nu\epsilon\} = \rho_0/2 + e \in H^{1/2}(\Gamma) \quad (2.7)$$

which, owing to the mapping properties of the single and double layer potential operators, satisfies

$$\|g\|_{H^{1/2}(\Gamma)} \leq c_1(\|\epsilon\|_{H^{-1/2}(\Gamma)} + \|\delta\|_{H^{1/2}(\Gamma)}). \quad (2.8)$$

Let $a \in H^1(\Omega)$ be the unique solution to the Dirichlet problem

$$\Delta a = \operatorname{div} D_{\mathcal{T}} e \quad \text{and} \quad a|_{\Gamma} = g|_{\Gamma}. \quad (2.9)$$

Then, there exists some $b \in H^1(\Omega)/\mathbb{R}$ with

$$D_{\mathcal{T}} e = Da + \operatorname{Curl} b \quad (2.10)$$

such that, for all $\eta \in H_0^1(\Omega)$,

$$\int_{\Omega} \operatorname{Curl} b \cdot D\eta \, dx = 0. \quad (2.11)$$

Similarly, we find some $\alpha, \beta \in H^1(\Omega)$ with $\alpha = 0$ on Γ such that

$$\sigma - \Sigma = D\alpha + \operatorname{Curl} \beta. \quad (2.12)$$

Since a, b, α , and β are solutions of Dirichlet or Neumann problems, we find a constant c_2 which depends only on Ω such that

$$\begin{aligned} & \|Da\|_{L^2(\Omega)} + \|Db\|_{L^2(\Omega)} + \|D\alpha\|_{L^2(\Omega)} + \|D\beta\|_{L^2(\Omega)} \\ & \leq c_2(\|g\|_{H^{1/2}(\Gamma)} + \|D_{\mathcal{T}} e\|_{L^2(\Omega)} + \|\sigma - \Sigma\|_{L^2(\Omega)}) \\ & \leq c_2(c_1\|\epsilon\|_{H^{-1/2}(\Gamma)} + c_1\|\delta\|_{H^{1/2}(\Gamma)} + (1 + C_A)\|D_{\mathcal{T}} e\|_{L^2(\Omega)}), \end{aligned} \quad (2.13)$$

where we used (2.8), $|\operatorname{Curl} \cdot| = |D \cdot|$, and the Lipschitz continuity of \mathcal{A} with Lipschitz constant C_A . According to the uniform monotonicity of \mathcal{A} , we consider

$$c_{\mathcal{A}}\|D_{\mathcal{T}} e\|_{L^2(\Omega)}^2 \leq (\sigma - \Sigma, D_{\mathcal{T}} e) = (\sigma - \Sigma, Da) + (D\alpha + \operatorname{Curl} \beta, \operatorname{Curl} b) \quad (2.14)$$

by (2.10) and (2.11). It is well-established that one can construct an approximant $A = \mathcal{I}a \in S^1$ with the following properties

$$\|a - \mathcal{I}a\|_{L^2(T)} \leq Ch_T \|Da\|_{L^2(\mathcal{N}(T))}, \quad (2.15)$$

$$\|a - \mathcal{I}a\|_{L^2(E)} \leq Ch_E^{1/2} \|Da\|_{L^2(\mathcal{N}(E))}, \quad (2.16)$$

for all $T \in \mathcal{T}$, $E \in \mathcal{E}$ (see, e.g., [5, 12]). Here, $\mathcal{N}(T)$ (resp. $\mathcal{N}(E)$) is the union of T and at most $\lfloor 2\pi/c_{\theta} \rfloor$ other elements which share a common node with T (resp. the union of at most two elements which share E as a common side). The constant $C > 0$ in (2.15)–(2.16) depends only on c_{θ} . For the proofs we refer to [12] and notice that (2.15)–(2.16) are improved in [5, 11].

Then, given A , we calculate with the exact and discrete equation

$$\begin{aligned} (\sigma - \Sigma, Da) &= (\sigma - \Sigma, D(a - A)) + (\sigma, DA) - (\Sigma, DA) \\ &= (\sigma - \Sigma, D(a - A)) - (\operatorname{div}\sigma, A) + \langle \sigma n, A \rangle - \langle \Phi + t_0, A \rangle - (f, A) \\ &= (\sigma - \Sigma, D(a - A)) + \langle \sigma n - \Phi + t_0, A \rangle \end{aligned}$$

with an integration by parts. Since $\sigma n = \partial v / \partial n + t_0 = \phi + t_0$ and by an elementwise integration by parts we obtain (recall that the skeleton $\cup \mathcal{E} \setminus \Gamma := (\cup \mathcal{E}) \setminus \Gamma$ is the union of all inner edges)

$$\begin{aligned} (\sigma - \Sigma, Da) &= (-\operatorname{div}\sigma + \operatorname{div}_{\mathcal{T}}\Sigma, a - A) - \int_{\cup \mathcal{E} \setminus \Gamma} J_n(a - A) ds \\ &\quad + \langle \sigma n - \Sigma n, a - A \rangle + \langle \epsilon, A \rangle \\ &= (f + \operatorname{div}_{\mathcal{T}}\Sigma, a - A) - \int_{\cup \mathcal{E} \setminus \Gamma} J_n(a - A) ds \\ &\quad - \langle \Sigma n - \Phi - t_0, a - A \rangle + \langle \epsilon, a \rangle \\ &= (f + \operatorname{div}_{\mathcal{T}}\Sigma, a - A) - \int_{\cup \mathcal{E}} J_n(a - A) ds + \langle \epsilon, a \rangle. \quad (2.18) \end{aligned}$$

By the approximation properties of A , we have (as, e.g., in [15])

$$\begin{aligned} (f + \operatorname{div}_{\mathcal{T}}\Sigma, a - A) - \int_{\cup \mathcal{E}} J_n(a - A) ds \\ \leq c_3 \left\{ \sum_{T \in \mathcal{T}} h_T^2 \|f + \operatorname{div}_{\mathcal{T}}\Sigma\|_{L^2(T)}^2 + \sum_{E \in \mathcal{E}} n_E^2 \right\}^{1/2} \|Da\|_{L^2(\Omega)}. \quad (2.19) \end{aligned}$$

Since $\alpha = 0$ on Γ , the second contribution to the right-hand side of (2.14) is

$$(D\alpha + \operatorname{Curl} \beta, \operatorname{Curl} b) = (\operatorname{Curl} \beta, \operatorname{Curl} b) = (\operatorname{Curl} \beta, D_{\mathcal{T}}(e - a)). \quad (2.20)$$

Let $B := \mathcal{I}\beta \in S^1(\mathcal{T})$ be the Clément interpolant of β (which satisfies (2.15)–(2.16) as well). Then, $\partial B / \partial s \in S^0(\mathcal{G})$ and so $\langle \rho_0, \partial B / \partial s \rangle = 0$ and, using $\int_{E \setminus \Gamma} [U] ds = 0$ for all $E \in \mathcal{E}$,

$$\int_{\cup \mathcal{E} \setminus \Gamma} [U] \partial B / \partial s ds = 0 = \langle \rho_0, \partial B / \partial s \rangle. \quad (2.21)$$

Therefore, an elementwise integration by parts yields

$$\begin{aligned} \int_{\Omega} \operatorname{Curl} B \cdot D_{\mathcal{T}}(e - a) dx &= \int_{\cup \mathcal{E}} [e - a] \partial B / \partial s ds \\ &= \langle \partial B / \partial s, e - a \rangle = \langle \partial B / \partial s, \rho_0 / 2 \rangle = 0 \quad (2.22) \end{aligned}$$

(where we used $a = g$ on Γ and (2.7)). Employing (2.22) in (2.20) performing an elementwise integration by parts, we obtain

$$\begin{aligned} (D\alpha + \text{Curl } \beta, \text{Curl } b) &= (\text{Curl } (\beta - B), D_{\mathcal{T}}(e - a)) \\ &= - \int_{\cup \mathcal{E}} (\beta - B) \partial(e - a) / \partial s \, ds \\ &\leq c_4 \left(\|h_E^{1/2} [\partial U / \partial s]\|_{L^2(\cup \mathcal{E} \setminus \Gamma)} + \|h_E^{1/2} \partial \rho_0 / \partial s\|_{L^2(\Gamma)} \right) \|D\beta\|_{L^2(\Omega)}, \end{aligned} \quad (2.23)$$

owing to the approximation properties of the Clément interpolation and a trace estimate (cf., e.g., [15]). Note that $\rho_0 = 2U - 2u_0 + \mathcal{V}\Phi - (\mathcal{K} + 1)\Xi$. Let η^2 denote the right-hand side of (2.3) and observe that (2.14), (2.18), (2.19), (2.23), and $a = g$ on Γ verify

$$c_A \|D_{\mathcal{T}} e\|_{L^2(\Omega)} \leq c_5 \eta (\|Da\|_{L^2(\Omega)} + \|D\beta\|_{L^2(\Omega)}) + \langle \varepsilon, g \rangle. \quad (2.24)$$

A small calculation (which uses that \mathcal{K} and \mathcal{K}^* are adjoint) leads to

$$\begin{aligned} 2\langle \varepsilon, g \rangle &= \langle \varepsilon, (\mathcal{K} + 1)\delta - \mathcal{V}\varepsilon \rangle = \langle (\mathcal{K}^* + 1)\varepsilon, \delta \rangle - \langle \varepsilon, \mathcal{V}\varepsilon \rangle \\ &= \langle \rho_1, \delta \rangle - \langle \delta, \mathcal{W}\delta \rangle - \langle \varepsilon, \mathcal{V}\varepsilon \rangle, \end{aligned} \quad (2.25)$$

and we deduce in (2.24) that, owing to the positive definiteness of \mathcal{V} and \mathcal{W} ,

$$\begin{aligned} c_6 \{ \|D_{\mathcal{T}} e\|_{L^2(\Omega)}^2 + \|\delta\|_{H^{1/2}(\Gamma)/\mathbb{R}}^2 + \|\varepsilon\|_{H^{-1/2}(\Gamma)}^2 \} \\ \leq \eta (\|Da\|_{L^2(\Omega)} + \|D\beta\|_{L^2(\Omega)}) + \|\rho_1\|_{H^{-1/2}(\Gamma)} \|\delta\|_{H^{1/2}(\Gamma)/\mathbb{R}}. \end{aligned} \quad (2.26)$$

Finally, absorb the term $\|\delta\|_{H^{1/2}(\Gamma)/\mathbb{R}}$ on the right-hand side, recall from [4] (or [2] in Part I) that

$$\|\rho_1\|_{H^{-1/2}(\Gamma)} \leq c_7 \|h_{\mathcal{E}}^{1/2} \rho_1\|_{L^2(\Gamma)} = c_7 \|h_{\mathcal{E}}^{1/2} \{(\mathcal{K}^* + 1)\Phi + \mathcal{W}\Xi\}\|_{L^2(\Gamma)}, \quad (2.27)$$

and employ (2.13) to conclude the proof. \square

Remark 1. A more precise analysis of inequality (2.19) is given in [6] where c_3 is estimated analytically and in [7] a numerical approach is shown to approximate c_3 .

Remark 2. The volume contribution in (2.3) can be omitted. Indeed, for a modification $\tilde{A} \in S^1(\mathcal{T}) \subseteq S^{NC}(\mathcal{T})$ of the Clément-interpolation to a it can be shown

that, in addition to (2.19),

$$\begin{aligned} (f + \operatorname{div}_T \Sigma, a - \tilde{A}) - \int_{\cup \mathcal{E}} J_n(a - \tilde{A}) ds \\ \leq c_8 \left\{ \sum_{z \in \mathcal{N}} h_z^2 \|f - f_{\omega_z}\|_{L^2(\omega_z)}^2 + \sum_{E \in \mathcal{E}} n_E^2 \right\}^{1/2} \|Da\|_{L^2(\Omega)}. \end{aligned}$$

Here, \mathcal{N} denotes the set of all nodes, ω_z is the union of elements $T \in \mathcal{T}$ with the vertex z and f_{ω_z} is the integral mean of f on ω_z (see [5, 11]). Hence, in (2.3), $\|h_T f\|_{L^2(\Omega)}$ can be replaced by $\|h_T^2 Df\|_{L^2(\Omega)}$ which, generically, is of higher order and so negligible.

3. Efficiency

Theorem 1 yields the a posteriori error estimate (1.3), where

$$\begin{aligned} \eta(T)^2 := h_T^2 \int_T |f + \operatorname{div}_T \Sigma|^2 dx + \sum_{E \in \mathcal{E} \wedge E \subset \partial T} h_E (\|J_n\|_{L^2(E)}^2 \\ + \|J_\tau\|_{L^2(E)}^2 + \|\mathcal{W}\Xi + (\mathcal{K}^* + 1)\Phi\|_{L^2(E \cap \Gamma)}^2). \end{aligned} \quad (3.1)$$

This global reliable estimate is sharp in the sense that, up to higher order approximation errors, the reverse inequality is true partly in a local form.

Let $\mathcal{N}(T)$ denote the union of all triangles that share one vertex with $T \in \mathcal{T}$ and let $\mathcal{N}(E)$ denote the union of at most two triangles that share $E \in \mathcal{E}$ as an element side.

Theorem 2. *Suppose $\Sigma \in S_h^0(\Omega)$ and let f_T denote the integral mean of f on $T \in \mathcal{T}$. Let $\hat{u} \in \mathcal{S}^1(T)$ approximate u in $H^1(\Omega)$, while \tilde{t}_0 resp. $\tilde{\phi} \in \mathcal{S}^0(\mathcal{G})$ approximates t_0 resp. ϕ in $L^2(\Gamma)$ and $\tilde{\xi} \in \mathcal{S}^1(\mathcal{G})$ approximates ξ in $H^1(\Gamma)$. Then, there are constants $C_a, C_b > 0$ (which depend only on c_θ) such that*

$$\begin{aligned} C_a \eta(T)^2 &\leq \|\sigma - \Sigma\|_{L^2(\mathcal{N}(T))}^2 + \|h_T(f - f_T)\|_{L^2(\mathcal{N}(T))}^2 \\ &\quad + \|h_\mathcal{E}^{1/2}(t_0 - \tilde{t}_0)\|_{L^2(\Gamma \cap \partial T)}^2 + \|h_\mathcal{E}^{1/2}(\phi - \Phi)\|_{L^2(\Gamma \cap \partial T)}^2 \\ &\quad + \|h_\mathcal{E}^{1/2} \frac{\partial}{\partial s}(u - \hat{u})\|_{L^2(\Gamma \cap \partial T)}^2 + \|h_T^{1/2} D_T(u - \hat{u})\|_{L^2(\mathcal{N}(T))}^2 \\ &\quad + \|h_\mathcal{E}^{1/2} \mathcal{W}(\xi - \Xi)\|_{L^2(\Gamma \cap \partial T)}^2 + \|h_\mathcal{E}^{1/2}(\mathcal{K}^* - 1)(\phi - \Phi)\|_{L^2(\Gamma \cap \partial T)}^2 \\ &\quad + \|h_\mathcal{E}^{1/2} \frac{\partial}{\partial s} \mathcal{V}(\phi - \Phi)\|_{L^2(\Gamma \cap \partial T)}^2 + \|h_\mathcal{E}^{1/2} \frac{\partial}{\partial s}(\mathcal{K} - 1)(\xi - \Xi)\|_{L^2(\Gamma \cap \partial T)}^2 \end{aligned}$$

for each $T \in \mathcal{T}$ and

$$\begin{aligned} C_b \sum_{T \in \mathcal{T}} \eta(T)^2 &\leq \|\sigma - \Sigma\|_{L^2(\Omega)}^2 + \|h_{\mathcal{T}}(f - f_T)\|_{L^2(\Omega)}^2 + \|h_{\varepsilon}^{1/2}(t_0 - \tilde{t}_0)\|_{L^2(\Gamma)}^2 \\ &\quad + \|h_{\varepsilon}^{1/2} \frac{\partial}{\partial s}(u - \hat{u})\|_{L^2(\Gamma)}^2 + \|h_T^{1/2} D_{\mathcal{T}}(u - \hat{u})\|_{L^2(\Omega)}^2 \\ &\quad + h_{\Gamma, \max}/h_{\Gamma, \min} \left(\|\xi - \Xi\|_{H^{1/2}(\Gamma)}^2 + h_{\Gamma, \max} \left\| \frac{\partial}{\partial s}(\xi - \tilde{\xi}) \right\|_{L^2(\Gamma)}^2 \right) \\ &\quad + h_{\Gamma, \max}/h_{\Gamma, \min} \left(\|\phi - \Phi\|_{H^{-1/2}(\Gamma)}^2 + h_{\Gamma, \max} \|\phi - \tilde{\phi}\|_{L^2(\Gamma)}^2 \right). \end{aligned}$$

Proof: Arguing as in [15, (1.23)] we estimate $\|f_T\|_{L^2(T)}$ and obtain

$$3/\sqrt{20} \|h_T f_T\|_{L^2(T)} \leq \|h_T(f - f_T)\|_{L^2(T)} + c_9 \|\sigma - \Sigma\|_{L^2(T)}. \quad (3.2)$$

(The constant $c_9 > 0$ as well as c_{10}, \dots, c_{23} below depend only on c_{θ} [15, Lemma 1.3 and Eqn. (1.23)].)

Suppose that $E \in \mathcal{E}$ with $\mathcal{N}(E) := T_1 \cup T_2$ is the union of two triangles $T_1, T_2 \in \mathcal{T}$ sharing the common side E . Define $b_E := 4\lambda_{T_j,1} \lambda_{T_j,2}$ on T_j , $j = 1, 2$ and $b_E = 0$ on $\Omega \setminus \mathcal{N}(E)$. Here, $\lambda_{T,1}, \lambda_{T,2}, \lambda_{T,3}$ are the barycentric coordinates of $T \in \mathcal{T}$ and $\lambda_{T_j,1}$ and $\lambda_{T_j,2}$ are such that b_E is nonzero along E .

Let $E \in \mathcal{E}$ be an inner face, i.e., $E = T \cap T'$ for some $T' \in \mathcal{T}$, then using the extension operator $P : C(E) \rightarrow C(\mathcal{N}(E))$ from [15], we infer

$$\begin{aligned} \|J_n\|_{L^2(E)}^2 &= c_{10} \int_E b_E P(J_n) J_n \, ds \\ &= c_{10} \int_{\mathcal{N}(E)} \{D(b_E P(J_n))\Sigma + b_E P(J_n) \operatorname{div} \Sigma\} \, dx. \end{aligned} \quad (3.3)$$

Because of the inverse estimate and integration by parts we have

$$\|D(b_E P(J_n))\|_{L^2(\mathcal{N}(E))} \leq c_{11} h_E^{-1} \|b_E P(J_n)\|_{L^2(\mathcal{N}(E))} \quad \text{and}$$

$$\int_{\mathcal{N}(E)} \{D(b_E P(J_n))\sigma + b_E P(J_n) \operatorname{div} \sigma\} \, dx = 0.$$

Then, Cauchy's inequality, $\|b_E P(J_n)\|_{L^2(\mathcal{N}(E))} \leq c_{12} h_E^{1/2} \|J_n\|_{L^2(E)}$ and (3.3) lead to

$$h_E^{1/2} \|J_n\|_{L^2(E)} \leq c_{13} \left\{ \|\Sigma - \sigma\|_{L^2(\mathcal{N}(E))} + \|h_{\mathcal{T}}(f - f_T)\|_{L^2(\mathcal{N}(E))} \right\}. \quad (3.4)$$

Let $E \in \mathcal{G}$ be an edge on the boundary, $E \subset \Gamma$, and consider

$$\begin{aligned} h_E \int_E J_n^2 ds &= h_E \int_E |\Sigma \cdot n_E - \Phi - t_0|^2 ds \\ &\leq 2h_E \int_E |\Sigma \cdot n_E - \Phi - \tilde{t}_0|^2 ds + 2h_E \int_E |t_0 - \tilde{t}_0|^2 ds, \end{aligned} \quad (3.5)$$

where \tilde{t}_0 is the integral mean of t_0 on E . Arguing in the same way for $(\sigma - \Sigma) \cdot n$ in $\Sigma \cdot n - \Phi - t_0 = \epsilon - (\sigma - \Sigma) \cdot n$, $\epsilon := \phi - \Phi$, we obtain for $E \in \mathcal{G}$, (i.e., $E \subseteq \Gamma$) and $q := b_E P(\Sigma \cdot n_E - \Phi - \tilde{t}_0)$ that

$$\begin{aligned} h_E \int_E |\Sigma \cdot n_E - \Phi - \tilde{t}_0|^2 ds &= c_{10} h_E \int_E q(\Sigma \cdot n_E - \Phi - \tilde{t}_0) ds \\ &= c_{10} h_E \left(\int_E q(\Sigma - \sigma) \cdot n_E ds + \int_E q(\phi - \Phi) ds + \int_E q(t_0 - \tilde{t}_0) ds \right) \\ &\leq c_{10} h_E \int_{\mathcal{N}(E)} (\operatorname{div}_T(\sigma - \Sigma)q + (\sigma - \Sigma) \cdot Dq) dx \\ &\quad + c_{10} h_E \left(\|\epsilon\|_{L^2(E)} + \|t_0 - \tilde{t}_0\|_{L^2(E)} \right) \|q\|_{L^2(E)}. \end{aligned}$$

From $\|q\|_{L^2(\mathcal{N}(E))} \leq c_{12} h_E^{-1/2} \|\Sigma \cdot n_E - \Phi - \tilde{t}_0\|_{L^2(E)}$ and

$$\|Dq\|_{L^2(\mathcal{N}(E))} \leq c_{11} h_E^{-1} \|q\|_{L^2(\mathcal{N}(E))} \leq c_{11} c_{12} h_E^{-1/2} \|\Sigma \cdot n_E - \Phi - \tilde{t}_0\|_{L^2(E)},$$

it follows

$$\begin{aligned} h_E^{-1/2} \|\Sigma \cdot n_E - \Phi - \tilde{t}_0\|_{L^2(E)} &\leq c_{14} \left(\|h_T(f - \operatorname{div}_T \Sigma)\|_{L^2(\mathcal{N}(E))} \right. \\ &\quad \left. + \|\sigma - \Sigma\|_{L^2(\mathcal{N}(E))} + \|h_\varepsilon^{1/2} \epsilon\|_{L^2(E)} + \|h_\varepsilon^{1/2} (t_0 - \tilde{t}_0)\|_{L^2(E)} \right). \end{aligned} \quad (3.6)$$

With (3.2) and (3.5) this yields for $E = T \cap \Gamma$ that

$$\begin{aligned} h_E \int_E J_n^2 ds &\leq c_{15} \left(\|h_T(f - f_T)\|_{L^2(\mathcal{N}(T))}^2 \right. \\ &\quad \left. + \|\sigma - \Sigma\|_{L^2(\mathcal{N}(T))}^2 + \|h_\varepsilon^{1/2} \epsilon\|_{L^2(E)}^2 + \|h_\varepsilon^{1/2} (t_0 - \tilde{t}_0)\|_{L^2(E)}^2 \right). \end{aligned}$$

To prove the estimate

$$h_E \|J_\tau\|_{L^2(E)}^2 \leq c_{16} \|De\|_{L^2(\mathcal{N}(E))}^2 \quad (3.7)$$

for $E \in \mathcal{E}$, $E \not\subseteq \Gamma$, we argue as in [10, 14] and only illustrate the modified technique in case $E \in \mathcal{G}$ in the sequel. Note that $J_\tau = \partial/\partial s(2U - 2u_0 - (\mathcal{K} + 1)\Xi + \mathcal{V}\Phi) = \partial/\partial s(-2e + (\mathcal{K} + 1)\delta - \mathcal{V}\epsilon)$ because, as we mentioned in Part I [8], $2v|_\Gamma = (\mathcal{K} + 1)v - \mathcal{V}\phi$ as a consequence of the jump relations of the double layer potential. Since \hat{u} is affine on T ,

$$\begin{aligned} h_E \|J_\tau\|_{L^2(E)}^2 &\leq 3h_E \|(\mathcal{K} + 1)\delta - \mathcal{V}\epsilon\|_{H^1(E)}^2 \\ &\quad + 12h_E \|\partial/\partial s(U - \hat{u})\|_{L^2(E)}^2 + 12h_E |u - \hat{u}|_{H^1(E)}^2, \end{aligned}$$

where $|v|_{H^1(E)} := \|\partial v/\partial s\|_{L^2(E)}$ defines a semi-norm on $E \subseteq \Gamma$. We estimate the term $h_E \|\partial/\partial s(U - \hat{u})\|_{L^2(E)}^2$ as in the proof of (3.7) and calculate

$$\begin{aligned} &h_E \|\text{Curl}(U - \hat{u}) \cdot n_E\|_{L^2(E)}^2 \\ &= \frac{2}{3} h_E \text{Curl}(U - \hat{u}) \cdot n_E \int_E b_E \text{Curl}(U - \hat{u}) \cdot n_E ds \quad (3.9) \\ &= \frac{2}{3} h_E^{1/2} \|\text{Curl}(U - \hat{u}) \cdot n_E\|_{L^2(E)} \left| \int_T \text{div}(b_E \text{Curl}(U - \hat{u})) dx \right| \end{aligned}$$

thanks to Gauss' divergence theorem on $T \in \mathcal{T}$ with $E \subseteq \partial T$. Because $\text{div Curl} = 0$, we conclude from (3.9) that

$$\begin{aligned} h_E^{1/2} \|\partial/\partial s(U - \hat{u})\|_{L^2(E)} &\leq c_{17} \|D(U - \hat{u})\|_{L^2(T)} \quad (3.10) \\ &\leq c_{17} \left(\|De\|_{L^2(T)} + \|D(u - \hat{u})\|_{L^2(T)} \right). \end{aligned}$$

Using (3.5)–(3.10) we obtain

$$\begin{aligned} c_{18} \eta(T)^2 &\leq \|h_T(f - f_T)\|_{L^2(\mathcal{N}(T))}^2 + \|\sigma - \Sigma\|_{L^2(\mathcal{N}(T))}^2 \\ &+ \sum_{\substack{E \in \mathcal{E} \\ E \subseteq \partial T \cap \Gamma}} h_E \left(\|\epsilon\|_{L^2(E)}^2 + \|t_0 - \tilde{t}_0\|_{L^2(E)}^2 + |u - \hat{u}|_{H^1(E)}^2 + \|D_T(u - \hat{u})\|_{L^2(\mathcal{N}(T))}^2 \right. \\ &\quad \left. + |(\mathcal{K} + 1)\delta - \mathcal{V}\epsilon|_{H^1(E)}^2 + \|\mathcal{W}\delta + (\mathcal{K}^* + 1)\epsilon\|_{L^2(E)}^2 \right). \quad (3.11) \end{aligned}$$

(Notice equivalence of $\|\sigma - \Sigma\|_{L^2(T)}^2$ and $\|D_T e\|_{L^2(T)}^2$.) For the remaining part of this proof, let $|v|_{H^1(\Gamma)}$ denote the piecewise H^1 -semi-norm, i.e. $|v|_{H^1(\Gamma)}^2 :=$

$\sum_{E \in \mathcal{G}} \|\frac{\partial}{\partial \mathbf{s}} v\|_{L^2(E)}^2$. Summation over all $T \in \mathcal{T}$ leads to

$$\begin{aligned} c_{19} \sum_{T \in \mathcal{T}} \eta(T)^2 &\leq \|\sigma - \Sigma\|_{L^2(\Omega)}^2 + \|h_{\mathcal{T}}(f - f_T)\|_{L^2(\Omega)}^2 + \|h_{\mathcal{E}}^{1/2} \epsilon\|_{L^2(\Gamma)}^2 \\ &+ \|h_{\mathcal{E}}^{1/2}(t_0 - \tilde{t}_0)\|_{L^2(\Gamma)}^2 + |h_{\mathcal{E}}^{1/2}(u - \hat{u})|_{H^1(\Gamma)} + \|h_{\mathcal{T}}^{1/2} \mathcal{D}_{\mathcal{T}}(u - \hat{u})\|_{L^2(\Omega)} \\ &+ |h_{\mathcal{E}}^{1/2}((\mathcal{K} + 1)\delta - \mathcal{V}\epsilon)|_{H^1(\Gamma)}^2 + \|h_{\mathcal{E}}^{1/2}(\mathcal{W}\delta + (\mathcal{K}^* + 1)\epsilon)\|_{L^2(\Gamma)}^2. \end{aligned} \quad (3.12)$$

The terms $|h_{\mathcal{E}}^{1/2}(\mathcal{K} + 1)\delta|_{H^1(\Gamma)}$, $|h_{\mathcal{E}}^{1/2}\mathcal{V}\epsilon|_{H^1(\Gamma)}$, $\|h_{\mathcal{E}}^{1/2}\mathcal{W}\delta\|_{L^2(\Gamma)}$, and $\|h_{\mathcal{E}}^{1/2}(\mathcal{K}^* + 1)\epsilon\|_{L^2(\Gamma)}$ can be estimated exactly as in the conforming case, see [2] in Part I, and so we illustrate the arguments just for the first term. With $h_{\Gamma, \max(\min)} := \max(\min)_{E \in \mathcal{G}} h_E$ we have, according to the mapping properties,

$$\begin{aligned} |h_{\mathcal{E}}^{1/2}(\mathcal{K} + 1)\delta|_{H^1(\Gamma)}^2 &\leq c_{20} h_{\Gamma, \max} \|\delta\|_{H^1(\Gamma)}^2 \\ &\leq c_{20} h_{\Gamma, \max} (\|\xi - \tilde{\xi}\|_{H^1(\Gamma)}^2 + \|\tilde{\xi} - \Xi\|_{H^1(\Gamma)}^2) \end{aligned} \quad (3.13)$$

for any approximation $\tilde{\xi} \in \mathcal{S}^1(\mathcal{G})$ to $\xi = v|_{\Gamma}$. Then, thanks to well-established inverse estimates (see, e.g., [4] or [18] in Part I), we have

$$\begin{aligned} h_{\Gamma, \max} \|\tilde{\xi} - \Xi\|_{H^1(\Gamma)}^2 &\leq c_{21} h_{\Gamma, \max} / h_{\Gamma, \min} \|\tilde{\xi} - \Xi\|_{H^{1/2}(\Gamma)}^2 \\ &\leq 2c_{21} h_{\Gamma, \max} / h_{\Gamma, \min} (\|\xi - \Xi\|_{H^{1/2}(\Gamma)}^2 + \|\tilde{\xi} - \xi\|_{H^{1/2}(\Gamma)}^2). \end{aligned} \quad (3.14)$$

By the interpolation estimate and taking, e.g., $\tilde{\xi}$ as a nodal interpolant, we deduce

$$\|\tilde{\xi} - \xi\|_{H^{1/2}(\Gamma)}^2 \leq c_{22} h_{\Gamma, \max} \|\xi - \tilde{\xi}\|_{H^1(\Gamma)}^2. \quad (3.15)$$

Gathering (3.13)–(3.15) together, we are left with

$$\begin{aligned} |h_{\mathcal{E}}^{1/2}(\mathcal{K} + 1)\delta|_{H^1(\Gamma)}^2 \\ \leq c_{23} h_{\Gamma, \max} / h_{\Gamma, \min} (\|\xi - \Xi\|_{H^{1/2}(\Gamma)}^2 + h_{\Gamma, \max} \|\xi - \tilde{\xi}\|_{H^1(\Gamma)}^2). \end{aligned}$$

The remaining terms are estimated in the same way, so we neglect details. \square

Remark 3.1. The estimate (3.11) shows that $\eta(T)$ is a local estimator. Even for T at the interface Γ , the boundary contributions may be regarded as pseudo-local (according to the pseudo-locality of pseudo-differential operators).

Remark 3.2. The right-hand side consists of errors and of approximation errors. The latter terms are generically of higher order. This justifies the claim in the introduction that the a posteriori error estimate is generically efficient in case of a quasi-uniform mesh on the boundary.

4. Adaptive Algorithm and Implementation

Given a local error indicator $\eta(T)$ which is (even locally) related to the local error (in Theorem 2), we may follow the standard approach in residual based adaptive mesh-refining algorithms and obtain the following scheme.

Algorithm 4.1.

- (a) Start with a coarse mesh \mathcal{T} .
- (b) Solve the discrete problem for the actual mesh \mathcal{T} .
- (c) Compute $\eta(T)$ for all $T \in \mathcal{T}$.
- (d) Compute stopping criterion and decide to terminate or goto (e).
- (e) Refine the element T (red refinement) provided $\eta(T) \geq \frac{1}{2} \max_{T' \in \mathcal{T}} \eta(T')$.
- (f) Refine further elements (red-green-blue refinement) to avoid hanging nodes. Define resulting mesh as actual mesh \mathcal{T} , and go to (b).

For details on the red-green-blue refinement algorithms, we refer to [15] and only mention here that, thereby, the constant c_θ is uniformly bounded (with respect to the sequence of different meshes).

The adaptive algorithm is implemented in Matlab and we conclude this section with some remarks on the numerical Matlab-realisation before we present some numerical examples on the practical performance in the subsequent section.

We refer to Part I for details on the implementation of the discrete scheme. The calculation of the integrals for the residuals in (3.1) over the finite element T and the boundary element Γ_k is performed as follows. Since, in the following numerical examples \mathcal{A} in (1.1) is piecewise constant, and since U is piecewise affine, the jumps across the interior element boundaries in J_n and J_τ can be calculated exactly. The L^2 -Norm of

$$\mathcal{A}(D_{\mathcal{T}}U)|_T \cdot n_E - \Phi - t_0$$

is approximated via a 3-point Gaussian-quadrature formula on each boundary element Γ_k also the L^2 -Norm of

$$2DU|_T \cdot t_E - \partial/\partial s (2u_0 + (\mathcal{K} + 1)\Xi - \nu\Phi),$$

where for $x_i \in \Gamma_k$ and $g \in C(\Gamma_k)$ the derivative $\partial/\partial s g(x_i)$ is replaced by its central difference operator $[g(x_{i+1}) - g(x_{i-1})]/|x_{i+1} - x_{i-1}|$ with a distance of nodes $|x_{i+1} - x_{i-1}| = |\Gamma_k|/20$. The term

$$\int_{\Gamma_k} |\mathcal{W}\Xi + (\mathcal{K}^* + 1)\Phi|^2 ds$$

is approximated also with a 3-point Gaussian quadrature rule. Since $f = 0$ in the numerical examples the term $\int_T |f + \operatorname{div}_{\mathcal{T}} \mathcal{A}(D_{\mathcal{T}}U)|^2 dx$ vanishes.

Remark 4.1. The integral operators in (1.1) have to be tested only with piecewise polynomial functions. This can be done analytically and the code is fast and accurate. Also the terms in the a posteriori estimate (2.3) (except the integrals over the jumps u_0 and t_0) can be calculated analytically. Hence, compared with a posteriori error estimates for conforming finite elements [9] or [4] in Part I terms like $\mathcal{W}u_0$, $\mathcal{K}'t_0$ have not to be calculated. Since the given jumps u_0 and t_0 are general functions, these computations are in general difficult and cause a high amount of computational costs. Thus, for an adaptive approach in the case of conforming finite-elements and inhomogeneous jump conditions the coupling as introduced in this paper (see (1.1)) is preferable.

5. Numerical Examples

Two examples from Part I provide numerical evidence of the superiority of the adaptive mesh-refining Algorithm (A) in comparison with quasi-uniform mesh-refinement.

Table 1. Errors $|e_N|_{H^1(\Omega)}$ and error estimates η_N in Example 5.1

N	$ e_N _{H^1(\Omega)}$	η_N	$ e_N _{H^1(\Omega)}/\eta_N$
30	0.23819	1.86329	0.1278
77	0.23163	1.33962	0.1729
136	0.15752	0.86199	0.1827
195	0.11869	0.64563	0.1838
309	0.08863	0.49091	0.1805
472	0.06307	0.35315	0.1786
616	0.05308	0.29000	0.1830
985	0.04084	0.22146	0.1844
1417	0.03261	0.17459	0.1868
2210	0.02558	0.13760	0.1859
3397	0.02023	0.10864	0.1862
5077	0.01638	0.08756	0.1870
8288	0.01267	0.06783	0.1868

Example 5.1. The linear interface problem with $\mathcal{A} = \text{id}$ on the L-shaped domain shown in Fig. 1 of Part I has the exact solution $u(r, \theta) = r^{2/3} \sin(2/3\theta)$ in polar and Cartesian coordinates with a typical corner singularity. Hence, the convergence rate of the h-version with a uniform mesh does not lead to the optimal convergence rate even though the right-hand side is smooth.

The $L^2(\Omega)$ -Norm $D_{\mathcal{T}}(u - U)$ is calculated via the 7-point quadrature rule of order 6 from [1, Formula 25.4.63.c] on any triangle. Table 1 displays the numerical results for the meshes generated by Algorithm (A). We show the number of degrees of freedom N , the corresponding relative error e_N in the $H^1(\Omega)$ -semi-norm, the estimated error η_N and the ratio $|e_N|_{H^1(\Omega)}/\eta_N$. As in Part I we get experimentally a convergence of the form $O(h^\alpha)$ with a mesh size $h = O(N^{-1/2})$ and $\alpha = 2/3$ for

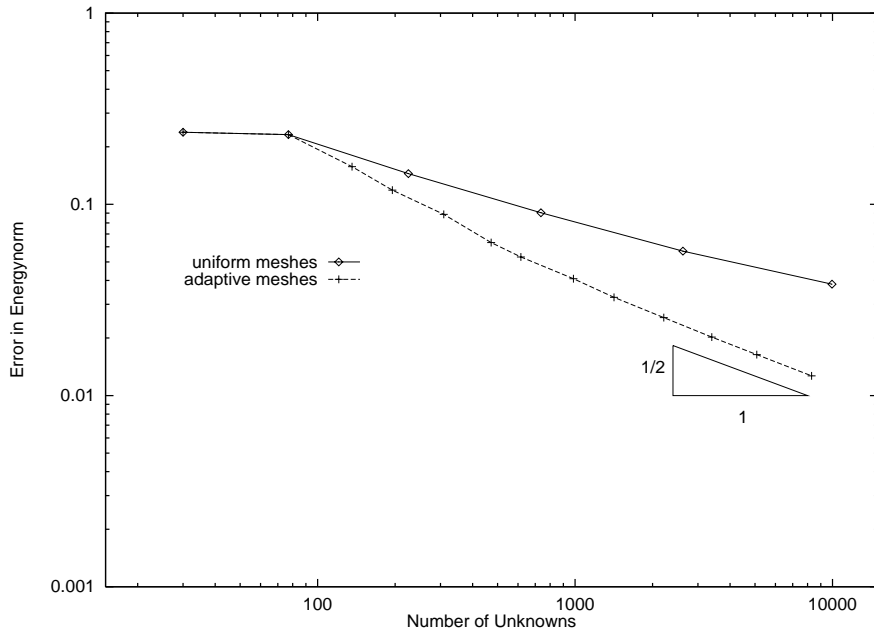


Figure 1. Errors $|e_N|_{H^1(\Omega)}$ for uniform and adaptive meshes

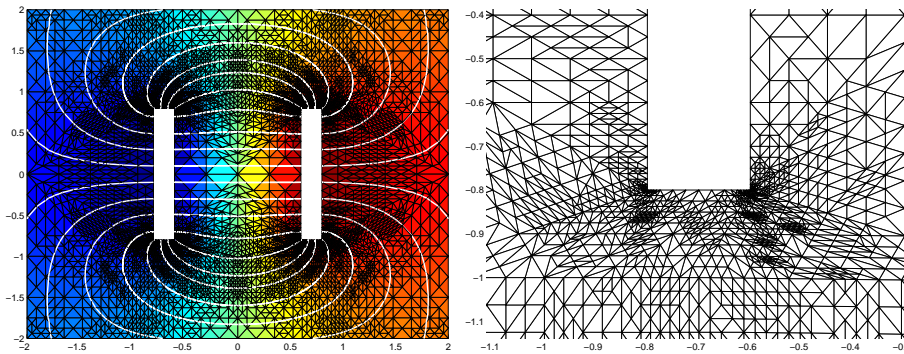


Figure 2. Solution (left) and zoom of the mesh (right) in Example 5.2

uniform meshes. For our adaptive approach we obtain quasi-optimal convergence rate which is approximately 1. (A slope $-1/2$ in Fig. 1 and 4 corresponds to an experimental convergence rate 1 owing to $N \propto h^{-2}$ in two dimensions.) The ratio $|e_N|_{H^1(\Omega)}/\eta_N$ has an upper bound (≤ 0.19) in our numerical example. This verifies the estimate (2.3) experimentally. The significant improvement of the convergence can be deduced from Fig. 1 where we plotted the error $u - U$ in H^1 -semi-norm for uniform and adaptive refinement versus the number of unknowns in a log-log-scale.

Example 5.2. The potential of a capacitor in an unbounded domain is computed with homogeneous jump conditions in (1.1) and $A = 5 \text{ id}$ with given charge ± 1 at

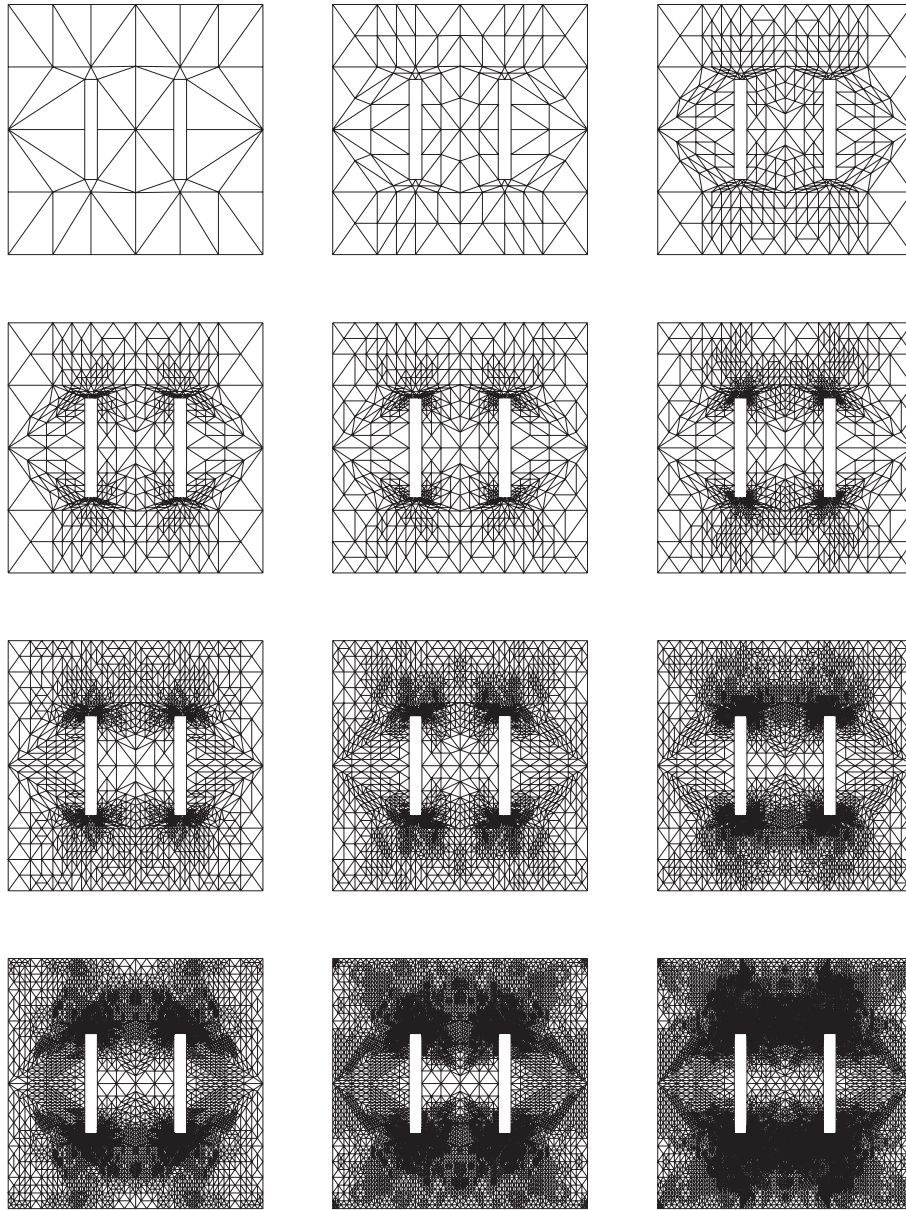


Figure 3. Sequence of adaptively refined meshes

boundaries $\Gamma_{D,1}$ and $\Gamma_{D,2}$. The geometry of Ω , Ω_c , Γ_C , $\Gamma_{D,\cdot}$ and the coarse grid is depicted in Fig. 2 of Part I.

Algorithm (A) produces a sequence of unstructured meshes as shown in Fig. 3. For the coarse mesh the problem behaves like a crack problem and as the mesh is more and more refined around $\Gamma_{D,j}$, it models a domain with re-entrant corners

of the Dirichlet boundary. The solution for this problem with $N = 21503$ and a magnification of the adaptively refined mesh around $\Gamma_{D,1}$ is provided in Fig. 2. The meshes are highly refined at corners of the Dirichlet boundary as expected. There is no additional refinement on the coupling boundary due to the coupling compared with pure FEM-modelling. As shown in Fig. 2 the refinement is symmetric to the x - and y -axis. The streamlines displayed give knowledge of gradients of the potential. Owing to the higher permeability in Ω the streamlines look more depressed and flat than in the case where $A = \text{id}$ as expected. Although we are using nonconforming finite elements (nc-FE) in Ω the streamlines appear smooth, also near the coupling boundary.

In Fig. 4 we plot the a posteriori error estimate η_N for uniform and adaptive meshes (from Fig. 3). The convergence rate of η_N is approximately 1 for the adaptive meshes and 0.72 for uniform meshes. As expected, the a posteriori error estimate η_N decreases faster for adaptively refined meshes with nearly optimal convergence rate.

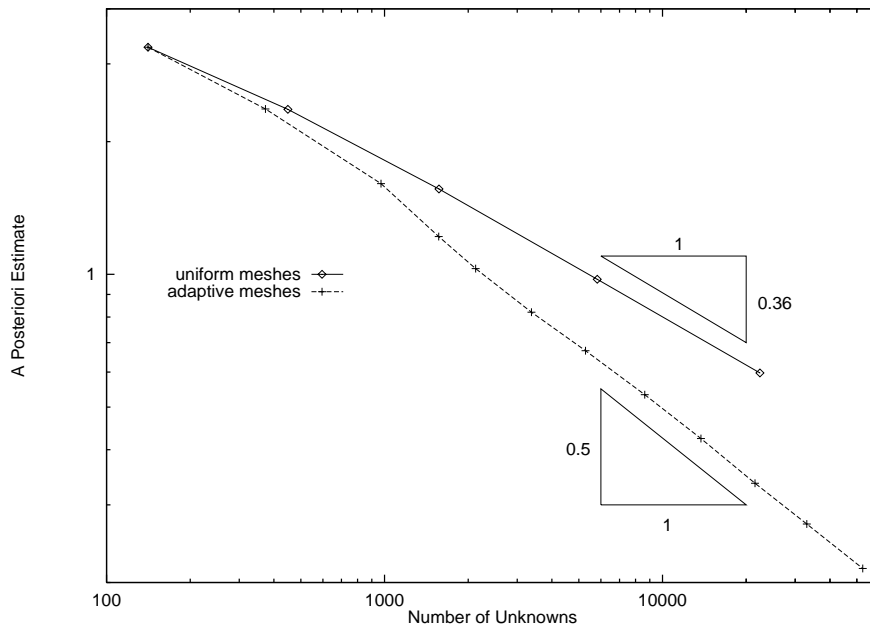


Figure 4. Error estimates η_N for uniform and adaptive meshes

From the numerical experiments, we deduce that adaptive methods are powerful tools for an efficient treatment of interface problems, especially within the coupling of nonconforming finite elements and boundary elements. The asymptotic convergence rates are improved to the optimal order and the considered error estimator is efficient and robust.

References

- [1] Abramowitz, M., Stegun, I. A.: Pocketbook of mathematical functions. Thun–Frankfurt/Main: Verlag Harri Deutsch 1984.
- [2] Alonso, A.: Error estimators for a mixed method. *Numer. Math.* 4, 385–395 (1996).
- [3] Carstensen, C.: A posteriori error estimate for the mixed finite element method. *Math. Comp.* 66, 465–476 (1997).
- [4] Carstensen, C.: Efficiency of a posteriori BEM error estimates for first kind integral equations on uniform meshes. *Math. Comp.* 65, 69–84 (1996).
- [5] Carstensen, C.: Weighted Clément-type interpolation and a posteriori analysis for FEM. Technical Report 97–19, Mathematisches Seminar, Christian-Albrechts-Universität zu Kiel (1997). M^2AN accepted for publication (1999).
- [6] Carstensen, C., Funken, S. A.: Constants in Clément-interpolation error and residual based a posteriori estimates in finite element methods. Technical Report 97–11, Mathematisches Seminar, Christian-Albrechts-Universität zu Kiel (1997).
- [7] Carstensen, C., Funken, S. A.: Fully reliable localised error control in the FEM. Technical Report 97–12, Mathematisches Seminar, Christian-Albrechts-Universität zu Kiel (1997). *SIAM J. Sc. Comp.* accepted for publication (1999).
- [8] Carstensen, C., Funken, S. A.: Coupling of nonconforming finite elements and boundary elements I: a priori estimates. *Computing* 62, 229–241 (1999).
- [9] Carstensen, C., Funken, S. A., Stephan, E. P.: On the coupling of FEM and BEM in 2–d–elasticity. *Num. Math.* 77, 187–221 (1997).
- [10] Carstensen, C., Jansche, S.: A posteriori error estimates and adaptive mesh-refining for non-conform finite element methods. Technical Report 97–8, Mathematisches Seminar, Christian-Albrechts-Universität zu Kiel (1997).
- [11] Carstensen, C., Verfürth, R.: Edge residuals dominate a posteriori error estimates for low order finite element methods. Technical report 97-6, Mathematisches Seminar, Christian-Albrechts-Universität zu Kiel (1997). *SIAM J. Numer. Anal.* accepted for publication (1998).
- [12] Clément, P.: Approximation by finite element functions using local regularization. *RAIRO Sér. Rouge Anal. Numér. R-2*, 77–84 (1975).
- [13] Dari, E., Duran, R., Padra, C.: Error estimators for nonconforming finite element approximations of the Stokes problem. *Math. Comp.* 64, 1017–1033 (1995).
- [14] Dari, E., Duran, R., Padra, C., Vampa, P.: A posteriori error estimators for nonconforming finite element methods. *Math. Modell. Numer. Anal.* 30, 385–400 (1996).
- [15] Verfürth, R.: A review of a posteriori error estimation and adaptive mesh-refinement techniques. Teubner: Wiley 1996.

Carsten Carstensen
Stefan A. Funken
Mathematisches Seminar
Christian-Albrechts-Universität zu Kiel
Ludewig-Meyn-Str. 4, D-24098 Kiel, Germany
e-mail: cc@numerik.uni-kiel.de
saf@numerik.uni-kiel.de